Photoluminescence study of the $In_{0.3}Ga_{0.7}As$ surface quantum dots coupling structure*

YANG Ying-li (杨莹丽)[1,2], **LIU Zeng-guang** (刘增光)[1], **WANG Guo-dong** (王国东)[1]**, **WANG Ying** (王颖)[3], **YUAN Qing** (苑青)[3], **and FU Guang-sheng** (傅广生)[3]

1. School of Physics and Electronic Information Engineering, Henan Polytechnic University, Jiaozuo 454000, China

2. Instrumental Analysis Center, Henan Polytechnic University, Jiaozuo 454000, China

3. College of Physics Science & Technology, Hebei University, Baoding 071002,China

(Received 24 June 2020; Revised 26 August 2020)

Photoluminescence (PL) was investigated as functions of the excitation intensity and temperature for a coupling surface quantum dots (SQDs) structure which consists of one $In_{0.3}Ga_{0.7}As$ SQDs layer being stacked on multi-layers of $In_{0.3}Ga_{0.7}As$ buried quantum dots (BQDs). Accompanied by considering the localized excitons effect induced by interface fluctuation, carrier transition between BQDs and SQDs were analyzed carefully. The PL measurements confirm that there is a strong carrier transition from BQDs to SQDs and this transition leads to obvious different PL characteristics between BQDs and SQDs. These results are useful for future application of SQDs as surface sensitive sensors.

Document code: A **Article ID:** 1673-1905(2021)05-0302-6

DOI https://doi.org/10.1007/s11801-021-0108-4

Self-assembled In(Ga)As/GaAs quantum dots (QDs) have achieved great success and have been incorporated in a wide range of optoelectronic devices, such as lasers, infrared detectors and solar cells etc[1-5]. It is believed that uncapped In(Ga)As surface quantum dots (SQDs) have potential applications in gas sensing because of their surface sensitive properties. A strong optical sensitivity to the surface environment has been reported for SQDs made of InAs and InGaAs[6-10]. Furthermore, under different light conditions, the relationship between the electrical response of InGaAs QDs nanostructures and the relative humidity of different environments have been careful analyzed[11]. In the above-mentioned works, the SQDs were obtained through directly deposited single layer QDs on the intrinsic buffer layer on the substrate. The sensitivity of SQDs to gases could be attributed to the existence of surface states in the SQDs and the adsorption of surface states on polar gases.

However, there are two issues that limit the application of SQDs on the gas sensing. One is the relatively poor photoluminescence (PL) performance due to the existence of surface states in the SQDs. The other is that the thickness of a single layer QDs is only a few nanometers. It is very difficult to make electrodes on such a thin layer of quantum dots to accurately measure the electrical response of the SQDs. Accordingly, the uniformity and the optical performance of QDs can be improved by desposited multi-layers QDs. For example, the multi-layers InAs/GaAs QDs was used to improving the performance of lasers[11,12] and solar cells[13,14]. Further, the optical performance of SQDs can be significantly improved by coupling structure in which the SQDs layer being stacked on multi-layer buried quantum dots (BQDs)[15-17]. In nano 0D or 1D material, carriers transferred have important influence on its optical property[18,19]. Similarly, in such coupling structures, carriers transferred to SQDs have important influence to improve PL efficiency and the gas sensitivity for SQDs. But the underlying mechanisms of coupling and carrier transfer related to SQDs are still not very clear and need to be investigated. In this work, a coupling SQDs structure is prepared which consists of one $In_{0.3}Ga_{0.7}As$ SQDs layer being stacked on multi-layer $In_{0.3}Ga_{0.7}As$ BQDs. The carrier transition between BQDs and SQDs is analyzed carefully by the temperature-dependent and excitation intensity-dependent PL measurements.

The coupling SQDs structure was grown by using a solid source molecular beam epitaxy (MBE) reactor on semi-insulating GaAs (001) substrates. The schematic diagram of the coupling structure is shown in Fig.1(a). The sample growth process has been described in detail elsewhere[20]. For comparison, a reference sample, that is the same five-layer $In_{0.3}Ga_{0.7}As$ BQDs structure without the final surface QDs, was also grown and characterized.

For PL measurements, the samples were mounted on the cold finger of a closed-cycle cryostat with temperature

* This work has been supported by the National Natural Science Foundation of China (Nos.U1304608 and 61774053), the Project of Henan Provincial Department of Science and Technology (No.182102410047), and the Program of Henan Polytechnic University (No.B2014-020).

** E-mail: wgd@hpu.edu.cn

variable between 10 K and 300 K. An excitation laser, operating at 532 nm, was focused on the sample surface to a spot size of a few micrometers in diameter by a 50× objective lens. The PL signal was dispersed by an Acton-50 cm spectrometer and then detected by a liquid-nitrogen cooled charge coupled device detector array. The purpose of depositing the etch stop layer and *Si* doping GaAs layer is to facilitate the fabrication of sensor electrodes in the future work.

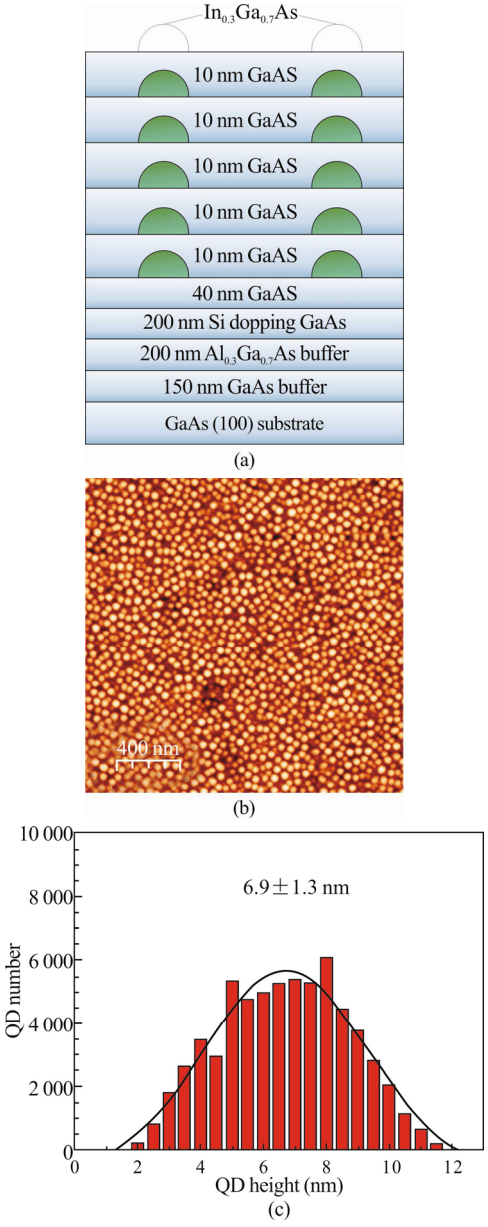

Fig.1 (a) Schematic of the stacking SQD structure; (b) 2 μm×2 μm AFM image of the SQDs; (c) Height distribution of SQDs

Fig.1(b) shows the 2 μm×2 μm atomic force microscope (AFM) image of the SQDs with the dot density estimated to be 3.8×10^{10} cm^{-2}, an average height of 6.9±1.3 nm, and an average diameter of 46±6 nm. No defects or large non-coherent islands are observed on the surface of the sample, indicating good QDs quality. The height distribution of SQDs are presented in the histogram of Fig.1(c), which showing a unimodal distribution. We noticed that the thickness of the GaAs capping layer is larger than average height of QDs. So the QDs in the BQDs layers are completely covered by GaAs. However, the QDs in the SQDs layers are entirely exposed due to the absence of Gas capping layer.

Low temperature (T=10 K) PL spectra were measured with a laser excitation intensity of 1 W/cm^2 for both the coupling structure and the reference sample. As plotted in Fig.2, there is a significant difference between these two samples. The reference sample shows a perfect Gaussian PL signal centered at 1 220 meV with a linewidth of 45.84 meV, which can be attributed to the fundamental electronic transition in the five layers of BQDs[20]. In comparison, PL spectrum of the coupling structure measured at 10 K with the same laser excitation intensity is shown in Fig.2(a) to have three prominent PL peaks. Gaussian fitting peaks to the spectrum are shown under the curves and the results are tabulated in the plot. The highest energy peak is centered at 1 220 meV with a linewidth of 47.76 meV. In consideration of BQDs PL peak from the reference sample, this highest energy peak is attributed to the emission from BQDs. The lowest energy peak, centered at 923.8 meV with a linewidth of 83.88 meV, is attributed to the emission from the SQDs. The SQDs peak is shifted to the red with respect to that of BQDs by about 296.2 meV, because the SQDs are not strained by a capping layer and thus approach to their natural lattice spacing and band gap[7,17].

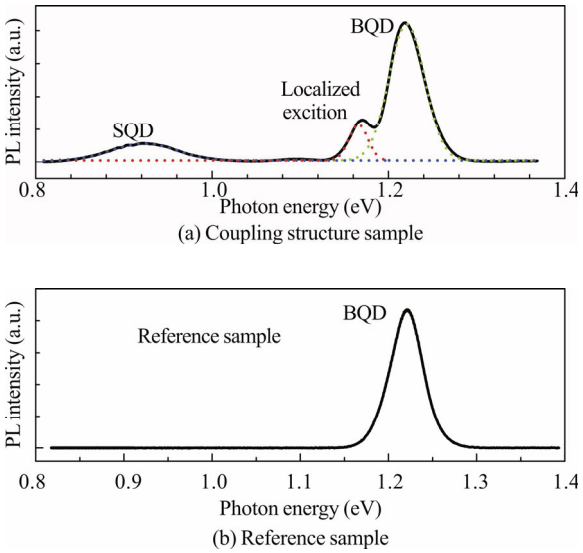

Fig.2 PL spectra measured at T=10 K

Interestingly, in this spectrum there is a small peak centered at 1 166 meV with a linewidth of 25.21 meV. Clearly, this small peak is not from the excited state emission of the BQDs because it is on the smaller-energy side of the BQDs peak. Large quantum dots or exciton effects would lead to such a small emission peak. However,

there is no multi-modal distribution of QDs height in AFM, as shown in Fig.1(c). Therefore, we suggest that this small peak is from the localized excitons. There are two ways to produce localized excitons. First, the $In_{0.3}Ga_{0.7}As$ QDs are covered completely by GaAs gap layer, forming the core-shell QDs. In this low dimension, the exciton effect enhancement significantly compared to that in bulk materials. Second, this small peak also can be from the localized excitons, which exhibit slightly lower energies due to potential modulations at the GaAs/InGaAs interface[16,17].

To prove our hypothesis, we then study the PL spectra at 10 K for the coupling structure sample and reference sample, respectively, as functions of excitation laser intensity between 0.01 W/cm^2 and 1 000 W/cm^2. The spectra, full width at half maximum (*FWHM*) and integrated PL intensity of coupling structure are presented in Fig.3. For the coupling structure, the *FWHM* of the three peaks have different excitation intensity dependences, as shown in the inset of Fig.3(a). The highest energy peak is from BQDs, its *FWHM* has little change as the excitation intensity is lower than 100 W/cm^2. Then it begins to increase with increasing excitation intensity. For the lowest energy peak emission from SQDs, its *FWHM* has similar excitation intensity dependent behaviors to that of the BQDs. But, the *FWHM* begins to increase at a excitation intensity of 1 W/cm^2. Compared with BQDs, the *FWHM* of SQDs begin to increase at a lower excitation intensity. This is a typical result in the BQDs and SQDs coupling structure. Because there is a carrier transition process from the BQDs to the SQDs, more carriers will prior to populate the SQDs than the BQDs[12]. We also observe that the *FWHM* of localized exciton peak decreases with increasing excitation intensity, coincident with the behaviors of localized exciton emission due to the interface fluctuation effect.

Fig.3(a) present PL spectra of the coupling structure sample. For convenience, each spectrum is normalized and shifted up according to the maximum PL intensity. As indicated by Fig.3(a), the profile of the PL spectrum from the coupling structure sample undergoes a transformation with increased excitation intensity. Under a weak excitation of 0.01 W/cm^2, it starts with a three peaks shape with the BQDs peak at highest energy side, the SQDs peak at lowest energy side, and the localized exciton peak besides the BQDs peak. As the excitation intensity is increased, the localized exciton peak becomes relatively inconspicuous. When the excitation intensity increases to 100 W/cm^2, the localized exciton peak disappears. Only the lower energy peak from SQDs and the higher energy peak from BQDs remain in the spectra. With further increasing excitation intensity, the PL spectra of BQDs become symmetric and a perfect Gaussian peak is visible. At the same time, the PL peak of SQDs becomes more and more weak relative to the BQDs.

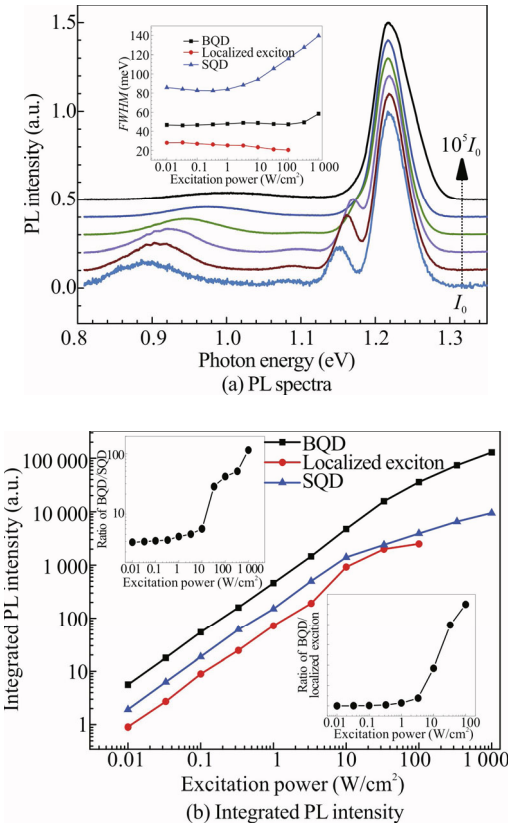

Fig.3 Spectra of coupling structure as a function of excitation intensity

The transformation of PL spectrum can be well explained. Although there are carriers transferred from BQDs to SQDs, as the excitation intensity increases, the SQDs tend to be saturated and more carriers will fill the BQDs to give a stronger BQDs peak. It can be further confirmed by the variation of the integrated PL intensity with respect to the excitation intensity, as illustrated in Fig.3(b) and its upper inset. After the excitation intensity increases to above 10 W/cm^2, the integrated PL intensity of SQDs become to increase slowly but the integrated PL intensity of BQDs still increase linearly. As a result, the integrated PL intensity ratio between BQDs and SQDs has a dramatically enhancement when the excitation intensity is greater than 10 W/cm^2.

We noticed that the peaks of SQDs and localized exciton exhibit a blueshift with the increased of excitation intensity. For SQDs, this abnormal PL behavior is likely the result of state filling in the QDs. Indeed, with a 532 nm excitation laser, the carriers are mainly generated inside the GaAs cap layer and then relax into the SQDs and the localized exciton before BQDs. Due to their different sizes the QDs have different probatilites to be populated by carriers. Therefore, the larger QDs have a larger carrier capture probability for weak excitation than the smaller dots. With increasing excitation intensity, the larger QDs begin to saturate and the smaller QDs have an increasingly higher probability to be populated. This

band filling result in an apparent blueshift. Similarly, due to their different sizes, the energy of localized excitons are also different, which leading to a blueshift of their peak wavelength with the increased of excitation intensity.

Further, the PL spectrum transformation of BQDs and SQDs also can be explained by the filling effect of the localized excitons and free excitons. At low excitation powers, the localized energy states are preferential populated, so a peak is clearly observed at lower energy side to correlate with the localized exciton emission. Then, with increasing excitation they are filled and get saturated quickly, because the state density of localized excitons is much lower in comparison with that of the free excitons. After the localized energy states become saturated, the free excitons emission remains its increasing with respect to the excitation intensity, finally becomes the dominant PL signal with a symmetric Gaussian profile. This can be confirmed by the trend of integrated PL intensities as functions of the excitation laser intensity, as shown in Fig.3(b) and the under inset. The integrated PL intensities from the SQDs, BQDs and localized excitons exhibit linear dependencies on the excitation intensity over three orders of magnitude from 0.01 W/cm^2 to 10 W/cm^2. Such linearity, only possible from high quality, low defect QDs structures, demonstrates that the PL emission is limited only by the carrier generation rate as determined by the excitation density. Further analysis in the underneath inset of Fig.3(b) shows that the integrated PL intensity ratio between the BQDs and localized excitons has minor change under excitation intensity lower than 1 W/cm^2, but increases significantly with excitation laser intensities stronger than that. This observation supports our hypothesis that the state density of localized excitons is much lower than that of the free excitons.

The normalized PL spectra, *FWHM* and integrated PL intensity of reference sample are extracted as functions of the excitation laser intensity at 10 K and plotted in Fig.4(a) and (b), respectively. As shown in Fig.4(a), there is only one Gaussian peak in PL spectrum of the reference sample as the excitation intensity increases from 0.01 W/cm^2 to 300 W/cm^2. This emission peak is from the BQDs layers reference sample. Its *FWHM* varies from 44.55 meV to 49.85 meV as the excitation intensity increases from 0.01 W/cm^2 to 300 W/cm^2, as shown in the inset of Fig.4(a), very smaller in comparison with that of BQDs in the coupling structure. When the excitation intensity further increases to 1 000 W/cm^2, the PL spectrum becomes asymmetric to have a shoulder peak from the excited states of BQDs.

Considering the identical growth conditions, the localized excitons emission should appear for both samples. However, there is no localized excitons peak observed in Fig.2(b) and Fig.4(a). We suppose that the localized excitons exist in both samples, but the state density of localized excitons is much lower than that of the free excitons. For the reference sample, the photo generated carriers were mainly captured by the BQDs and the free excitons emission from BQDs is dominant. The localized excitons emission is too weak to be observed. For the coupling structure sample, the photon-generated carriers will transfer from BQDs to SQDs and surface states. This reduces the BQDs emission to be comparable with the emission from localized excitons. As a result, the localized excitons peak appeared in Fig.2(a). This statement can be supported by carefully compare the integrated PL intensity with the excitation intensity increasing from 0.01 W/cm^2 to 1 000 W/cm^2. It increases approximately 6 orders for BQDs in the reference sample, while only 4 orders for BQDs in the coupling structure sample, as shown in Fig.4(b) and Fig.3(b), respectively.

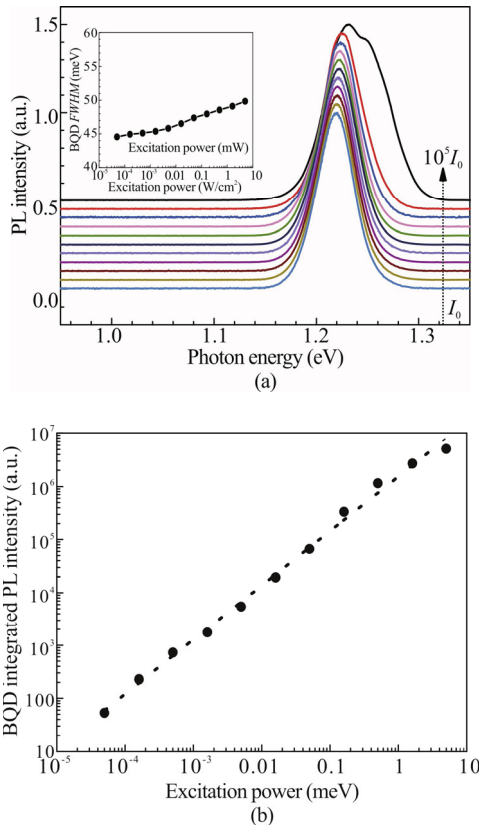

Fig.4 Spectra of reference sample as a function of excitation intensity: (a) PL spectra, where each spectrum is normalized to its maximum and shift up; (b) Integrated PL intensity

Figs.5 and 6 show the results of temperature dependent PL spectra measured with a excitation intensity of 30 W/cm^2. As shown in Fig.6(a), the reference sample has only one peak in the spectra as the temperature increases from 10 K to 300 K. The PL peak energy decrease from1.22 eV at 10 K to 1.15 eV at 300 K. This redshift is caused by the decreased QDs bandgap which can be predicted by the Varshni law. Similarly, for the coupling structure sample in Fig.5(a), the PL peak energy of

BQDs decreases from 1.2 eV to 1.15 eV and the PL peak energy of SQDs decreases from 0.95 eV to 0.91 eV, respectively, when the temperature increases from 10 K to 300 K.

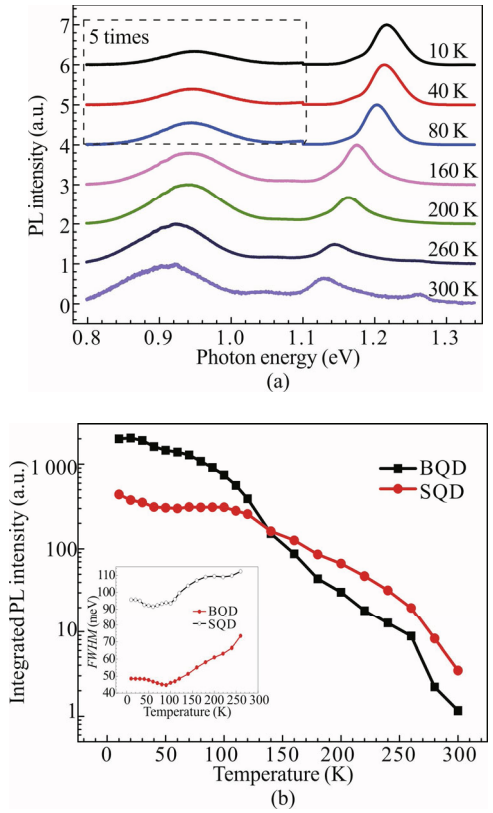

Fig.5 Spectra of coupling structure sample as a function of temperature: (a) PL spectra, where each spectrum is normalized to its maximum and shift up; (b) Integrated PL intensity

The insets of Fig.5(b) and Fig.6(b) demonstrate the variation of *FWHM* with respect to temperature for both samples. The *FWHM* of BQDs for the reference sample keeps broadening as the temperature increases from 10 K to 300 K due to phonon scattering. In our previous works[15], due to thermal activation and recapture of carriers, the *FWHM* of BQDs has a well-known narrowing behavior at the low temperature range. However, it did not occur in this work due to two possible reasons. One is that the excitation intensity is relatively high, and the other is that there is a doping layer under the BQDs layer. Both can provide enough carriers to BQDs layer. As a result, the carrier activation and recapture between the BQDs are relatively weak and the phonon scattering effect becomes prominent as the temperature increases.

For the coupling structure sample, the *FWHM* of the two QDs peaks have similar behaviors but different from that of reference sample. As shown in the set of Fig.5(b), the *FWHM* of BQDs and SQDs both become narrowing as the temperature increases. It is because that the carriers captured by the BQDs prefer to escape to SQDs via transferring rather than radiation recombination inside the BQDs. Also, in the SQDs layer, the carriers transferred from BQDs prefer to be captured by the large QDs. As results, the *FWHM* of BQDs and SQDs have a behavior of narrowing at low temperature range. When further increasing the temperature, the *FWHM* of both BQDs and SQDs increase as the thermal excitation of carriers out of the dots resulting in phonon broadening of the luminescence. From Fig.5(a),we noticed that there is a weak peak in the right of BQDs peak under 300 K and this weak peak disappeared quickly when the temperature decreased. Normally, it is believed that this weak peak is the luminescence of the wetting layer[21,22].

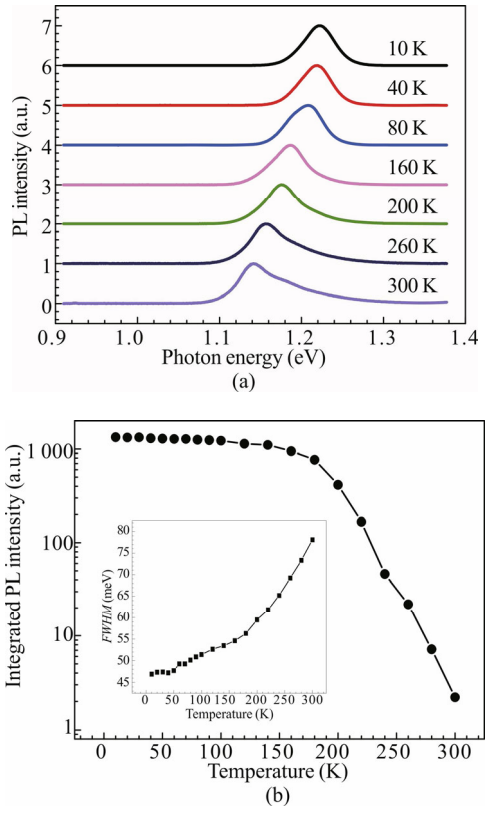

Fig.6 Spectra of reference sample as a function of temperature: (a) PL spectra, where each spectrum is normalized to its maximum and shift up; (b) Integrated PL intensity

We find in Fig.6(b) that the integrated PL intensity of the reference sample remains constant until the temperature rises to 160 K, then starts to quenching fast when the temperature further rise. The integrated PL intensity has decreased 3 orders when the temperature varied from 10 K to 300 K. This is a typical behavior for multilayer BQDs[12,15]. However, as shown in Fig.5(b), the SQDs PL peak and BQDs PL peak have totally different characterization. The integrated PL intensity of BQDs in coupling structure sample decreased also about 3 orders while it begins to quench at a very low temperature ~30 K. It is clear that the integrated PL intensity of BQDs in the coupling structure sample no longer remains constant but begins to quench at the range of

10—150 K. Consequently, the integrated PL intensity of SQDs in the coupling structure sample decreases slowly as the temperature rises from 10 K to 160 K, and it quench faster when the temperature rises further. We explain the temperature dependent behavior of the BQDs and SQDs in the coupling structure sample like this. Due to the thin spacer from the SQDs to BQDs layers, there is strong coupling between the SQDs and BQDs. This strong coupling leads to carriers transfer from the BQDs to SQDs. As a result, the integrated PL intensity of BQDs quench faster than that of SQDs although both of them decrease due to carrier thermal quenching.

In summary, the optical properties of a coupling structure sample and a reference sample were studied by temperature dependent and excitation intensity dependent PL measurements. The results show that there is a strong carrier transition from BQDs to SQDs in the coupling structure. The localized excitons induced by interface fluctuation also affect the carrier transition between BQDs and SQDs. This research has enriched the physical picture of carrier transition inside coupling structure and provided necessary information for device applications of SQDs as surface-sensitive sensors.

References

[1] Jinkwan Kwoen, Bongyong Jang, Joohang Lee, Takeo Kageyama, Katsuyuki Watanabe and Yasuhiko Arakawa, Optics Express **26**, 11568 (2018).

[2] Qizhu Li, Yuanqing Huang, Jiqiang Ning, Cheng Jiang, Xu Wang, Hongmei Chen, Xiao Li, Ruiying Zhang, Kai Zhang, Jiahua Min, Yong Peng and Ziyang Zhang, Nanoscale Research Letters **13**, 267 (2018).

[3] Dongyoung kim, Sabina Hatch, Jiang Wu, Kimberly A. Sablon, Phu Lam, Pamela Jurczak, Mingchu Tang, William P. Gillin and Huiyun Liu, IEEE Journal of Photovoltaics **8**, 741 (2018).

[4] Yves Bidaux, Ksenia A. Fedorova, Daniil A. Livshits, Edik U. Rafailov and Jerome Faist, IEEE Photonics Technology Letters **29**, 2246 (2017).

[5] Neil S. Beattie, Patrick See, Guillaume Zoppi, Palat M. Ushasree, Martial Duchamp, Ian Farrer, David A. Ritchie and Stanko Tomic, ACS Photonic **4**, 2745 (2017).

[6] Roberta De Angelis, Mauro Casalboni, Liliana D. Amico, Fabio De Matteis, Fariba Hatami, William T. Masselink and Paolo Prosposito, Key Engineering Materials **605**, 177 (2014).

[7] R. De Angelis, L. D'Amicro, M. Casalboni, F. Hatami, W. T. Masselink and P. Prosposito, Sensors and Actuators B: Chemical **189**, 113 (2013).

[8] R. De Angelis, M. Casalboni, F. Hatami, A. Ugur, W. T. Masselink and P. Prosposito, Sensors and Actuators B: Chemical B **162**, 149 (2012).

[9] M. J. Milla, J. M. Ulloa and A. Guzman, Applied Physics Letters **100**, 131601 (2012).

[10] Roberta De Angelis, Mauro Casalboni, Fabio De Matteis, Fariba Hatami, William T. Masselink, Hong Zhang and Paolo Prosposito, Journal of Luminescence **168**, 54 (2015).

[11] M. J. Milla, J. M. Ulloa and A. Guzman, Nanotehcnology **25**, 445501 (2014).

[12] B. L. Liang, Zh. M. Wang, Yu. I. Mazur and G. J. Salamo, Applied Physics Letters **89**, 243124 (2006).

[13] B. L. Liang, Zh. M. Wang, Yu. I. Mazur, Sh. Seydmohamadi, M. E. Ware and G. J. Salamo, Optics Express **15**, 8157 (2007).

[14] B. L. Liang, Yu I. Mazur, Vas P. Kunets, Zh. M. Wang, G. J. Salamo, E. A. Decuir Jr, B. Passmore and M. O. Manasreh, Nanotechnology **19**, 065705 (2008).

[15] G. Wang, B. L. Liang, B. C. Juang, A. Das, M. C Debnath, D. L. Huffaker, Y. I. Mazur, M. E. Ware and G. J. Salamo, Nanotechnology **27**, 465701 (2016).

[16] Y. Wang, X. Sheng, Q. Guo, X. Li, S. Wang, G. Fu, Y. I. Mazur, Y. Maidaniuk, M. E. Ware, G. J. Salamo, B. L. Liang and D. L. Huffaker, Nanoscale Research Letters **12**, 229 (2017).

[17] L. C. Pocas, E. M. Lopes, J. L. Durate, I. F. Dias, S. A. Lourenco, E. Laureto, M. Valadares, P. S. S. Guimaraes, L. A. Cury and J. C. Harmand, Journal of Applied Physics **97**, 103518 (2005).

[18] Fu Feng, Clementine Symonds, Catherine Schwob, Joel Bellessa, Agnes Maitre, Jean Paul Hugonin and Laurent Coolen, New Journal of Physic **20**, 033020 (2018).

[19] Fu Feng, Willy Daney de Marcillac, Xavier Lafosse, Simone Luca Portalupi, Michel Nasilowski, Benoit Dubertret, Jean Marc Frigerio, Catherine Schwob, Agnes Maitre, Pascale Senellart and Laurent Coolen, New Journal of Physic **20**, 083018 (2016).

[20] Gongdong Wang, Zengguang Liu, Junjun Wang, Yingli Yang, Xiaolian Liu, Xinran Zhang, Liwei Zhang and Guohua Cao, Photonic Sensors **10**, 283 (2020).

[21] Zhu Tian-Wei, Zhang Yuan-Chang, Xu Bo, Liu Feng-Qi and Wang Zhan-Guo, Acta Physica Sinica **52**, 2087 (2003). (in Chinese)

[22] Lu Zhendong, Xu Zhongying, Zheng Baozhen and Xu Jizong, Chinese Journal of Semiconductors **18**, 631 (1997).